

Supporting Information

Rational design of periodic porous Titanium Nitride MXene as multifunctional catalytic membrane

Tianqi Zhang, Zhaojian Zheng, Hao Lu, Hao Liu , Guobo Chen, Shuwei Xia, Long Zhou *, Meng Qiu *

Key Laboratory of Marine Chemistry Theory and Technology (Ocean University of China), Ministry of Education,
Qingdao 266100, China

*Correspondence and requests for materials should be addressed to drogonfly1988@126.com and
mengqiu@ouc.edu.cn

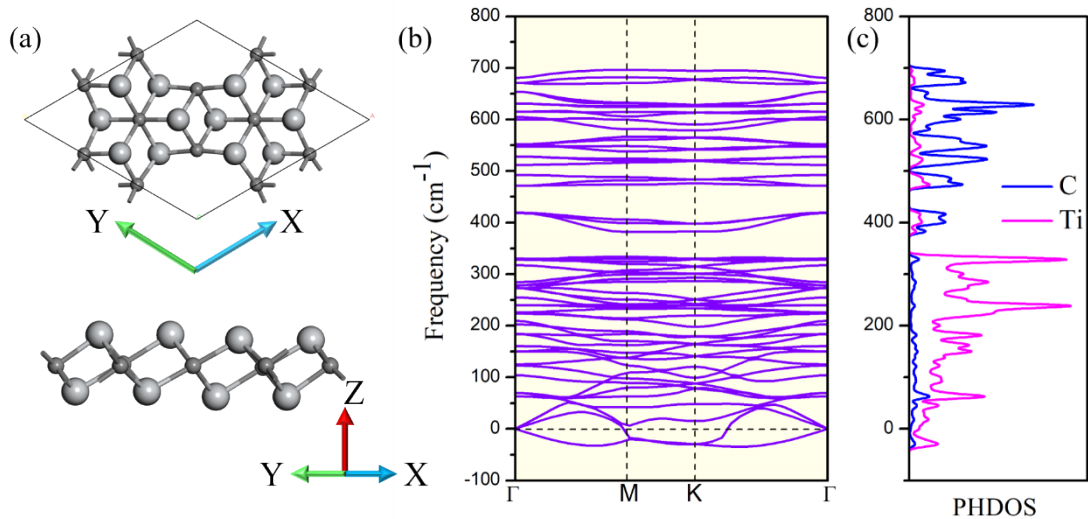


Fig. S1 Top and side view of optimized Ti_{12}C_8 (a), calculated phonon dispersion along the high symmetrical directions of the Brillouin zone (b) and the phonon PDOS (c). Little grey and big grey sphere represent carbon and titanium atom.

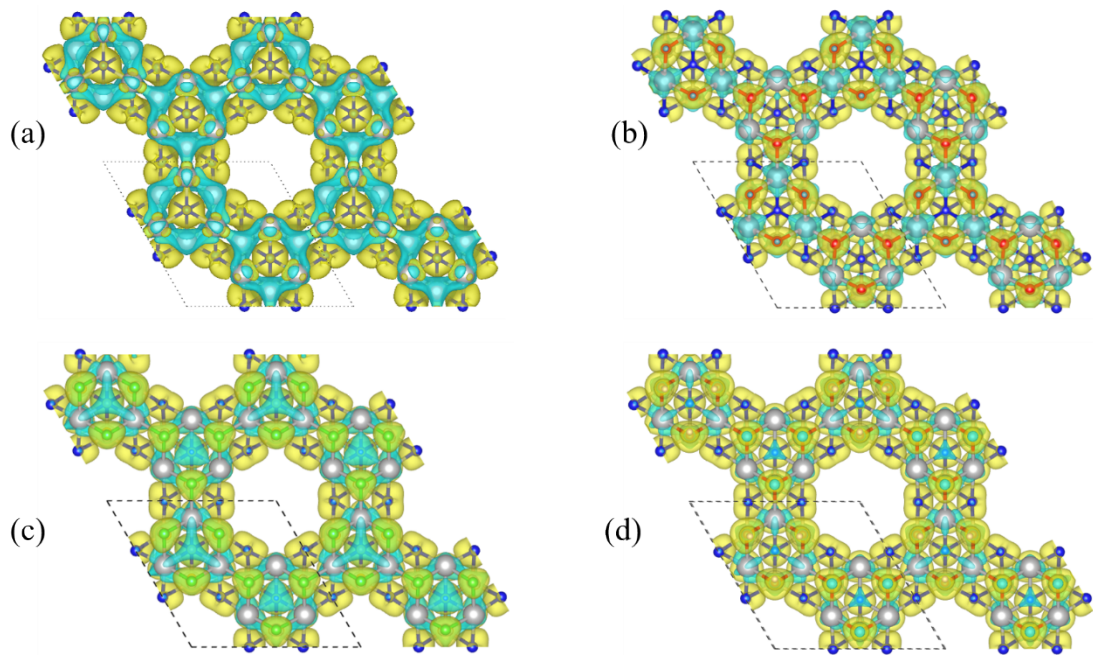


Fig. S2 Charge density difference of (a) Ti_{12}N_8 , (b) $\text{Ti}_{12}\text{N}_8\text{O}_{12}$, (c) $\text{Ti}_{12}\text{N}_8\text{F}_{12}$ and (d) $\text{Ti}_{12}\text{N}_8(\text{OH})_{12}$. Yellow zones represent electron accumulation and cyan zones are electron deficiency, isovalue =0.01 a.u.

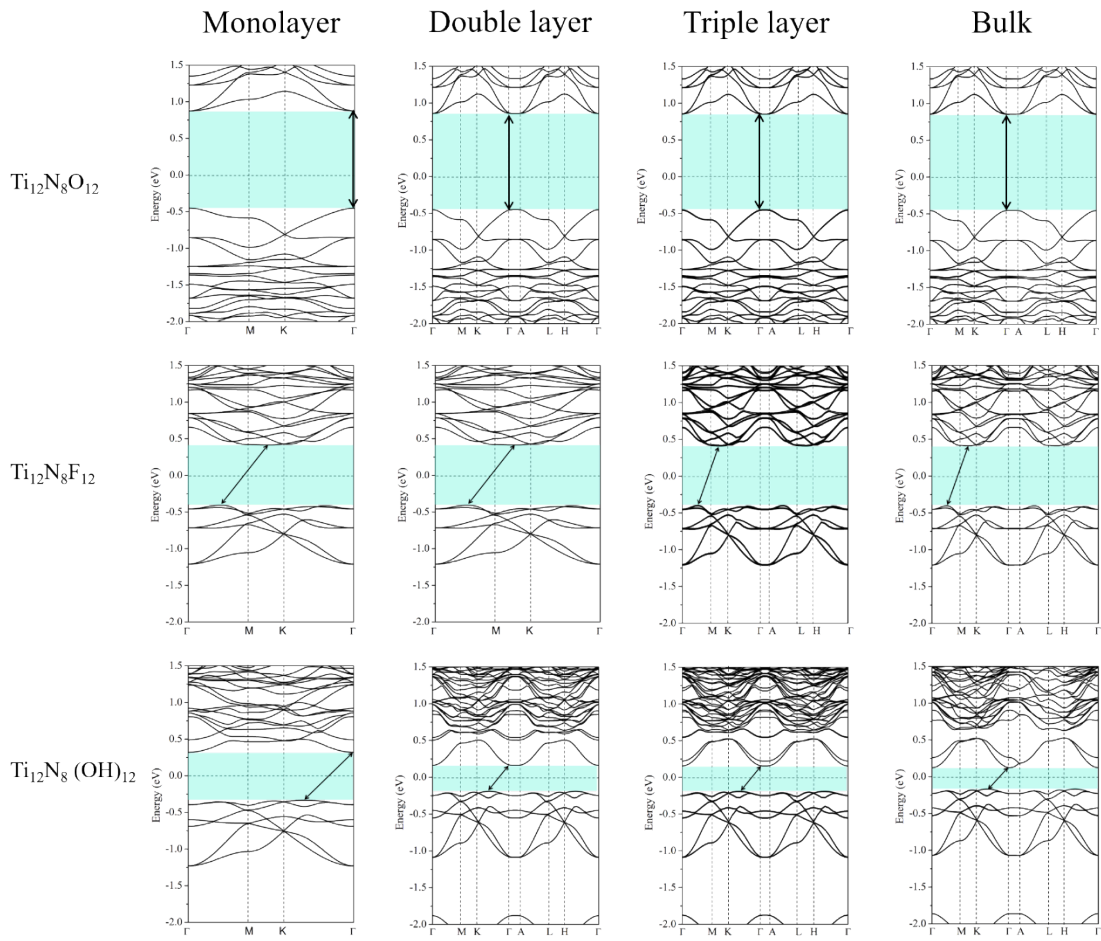


Fig. S3 Calculated band structure of the monolayer, bi-layer, triple layer and bulk of $\text{Ti}_{12}\text{N}_8\text{O}_{12}$, $\text{Ti}_{12}\text{N}_8\text{F}_{12}$ and $\text{Ti}_{12}\text{N}_8(\text{OH})_{12}$ by GGA/PBE

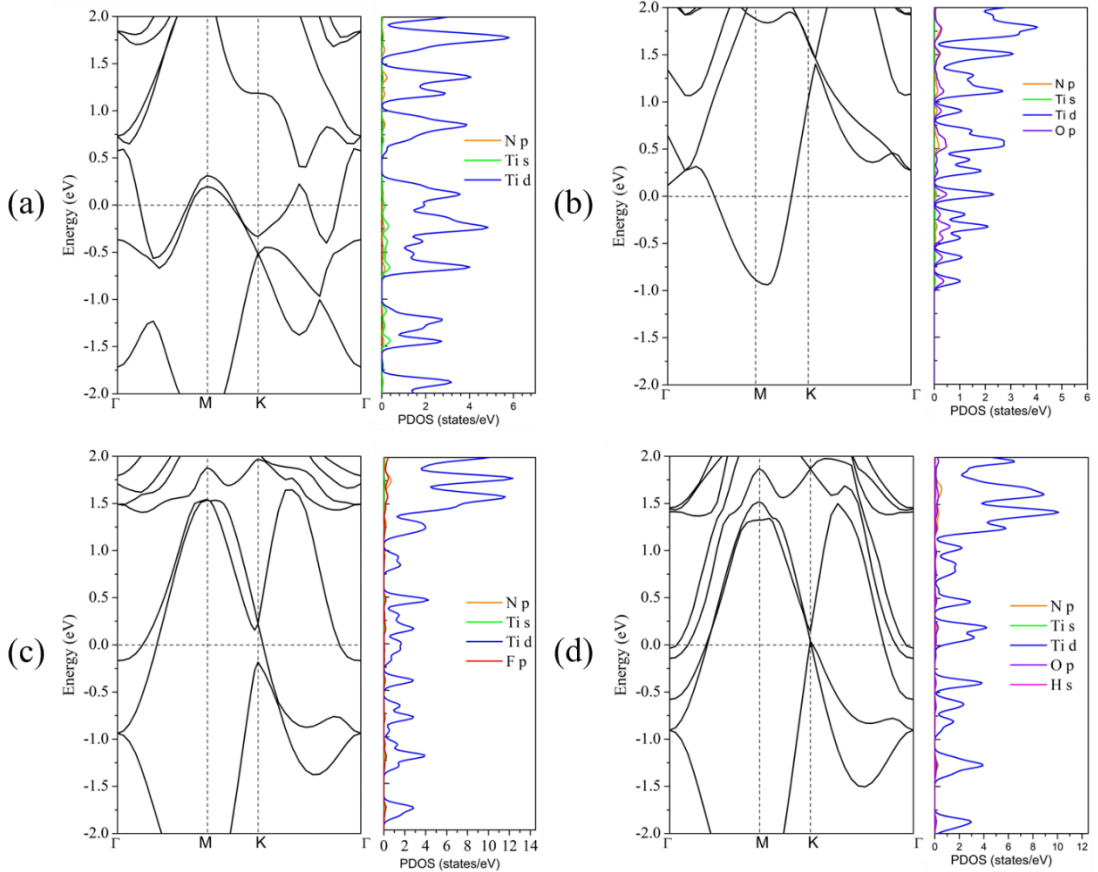


Fig. S4 Band structure (left) and density of states (right) of (a) Ti_2N , (b) Ti_2NO_2 , (c) Ti_2NF_2 and (d) $\text{Ti}_2\text{N}(\text{OH})_2$ under HSE06 theoretical level.

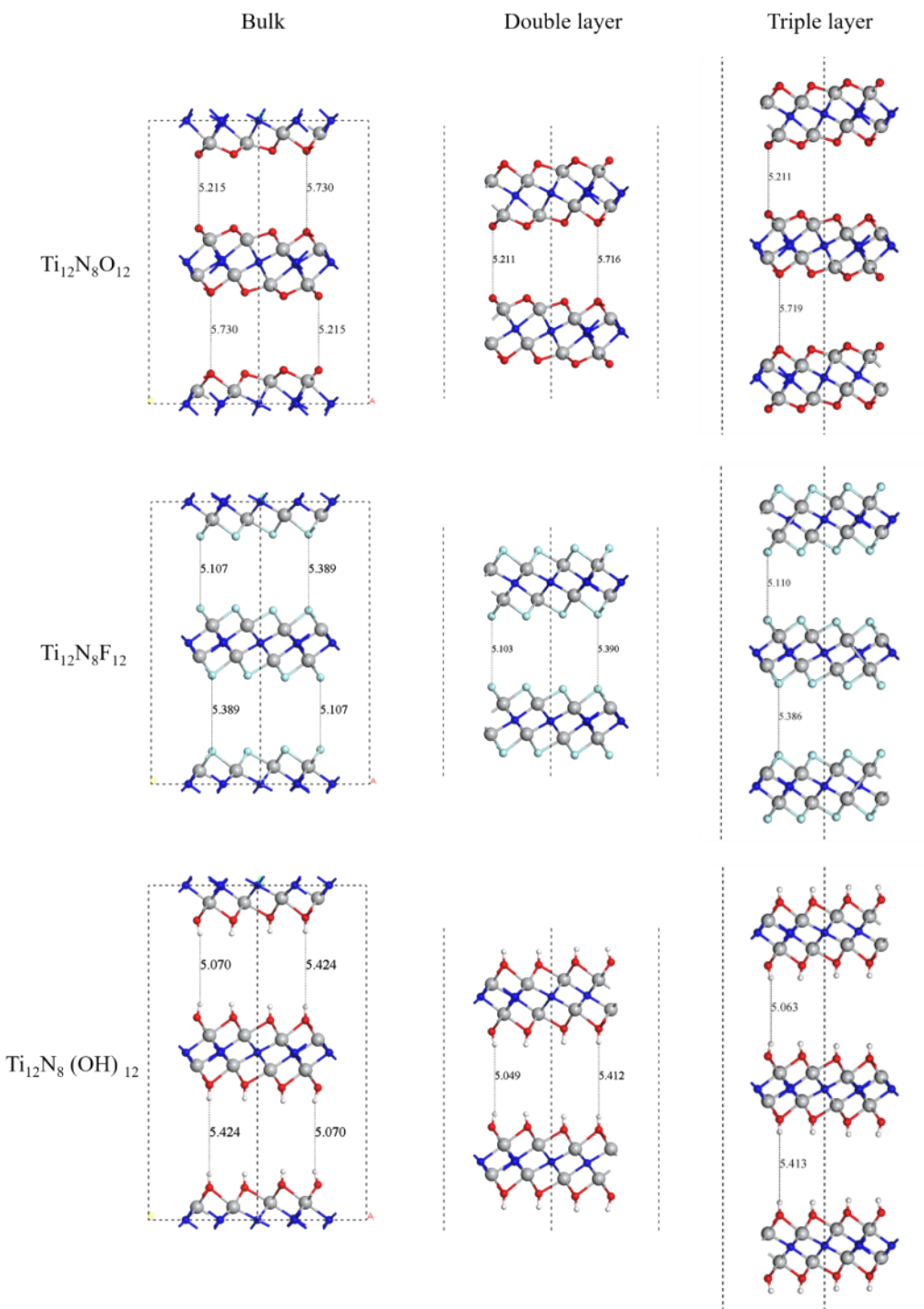


Fig. S5 Snapshot of bulk, bi-layer and triple layered $\text{Ti}_{12}\text{N}_8\text{O}_{12}$, $\text{Ti}_{12}\text{N}_8\text{F}_{12}$ and $\text{Ti}_{12}\text{N}_8(\text{OH})_{12}$.

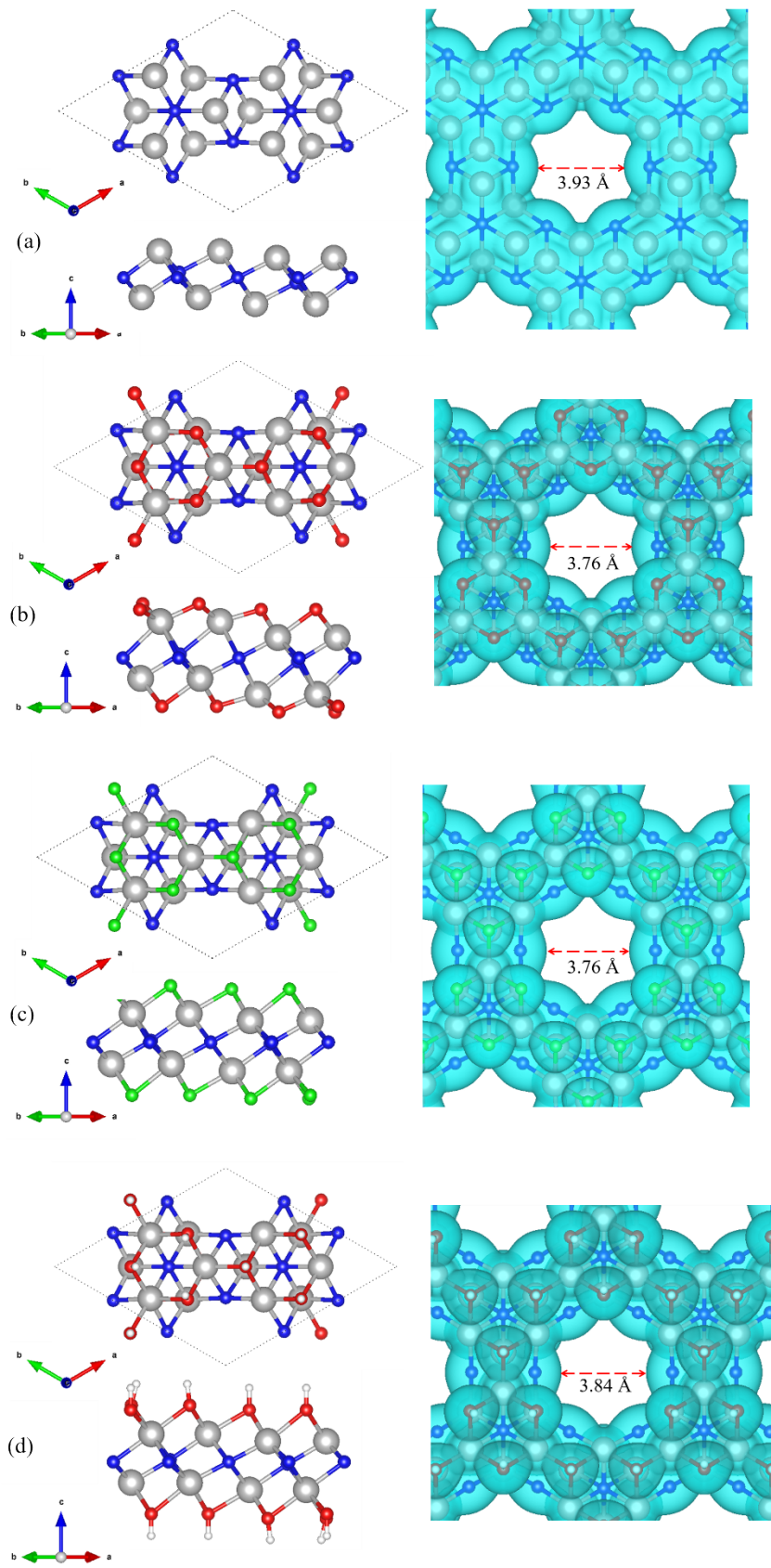


Fig.S6 Structure and electron density of (a) Ti_{12}N_8 , (b) $\text{Ti}_{12}\text{N}_8\text{O}_{12}$, (c) $\text{Ti}_{12}\text{N}_8\text{F}_{12}$ and (d) $\text{Ti}_{12}\text{N}_8(\text{OH})_{12}$

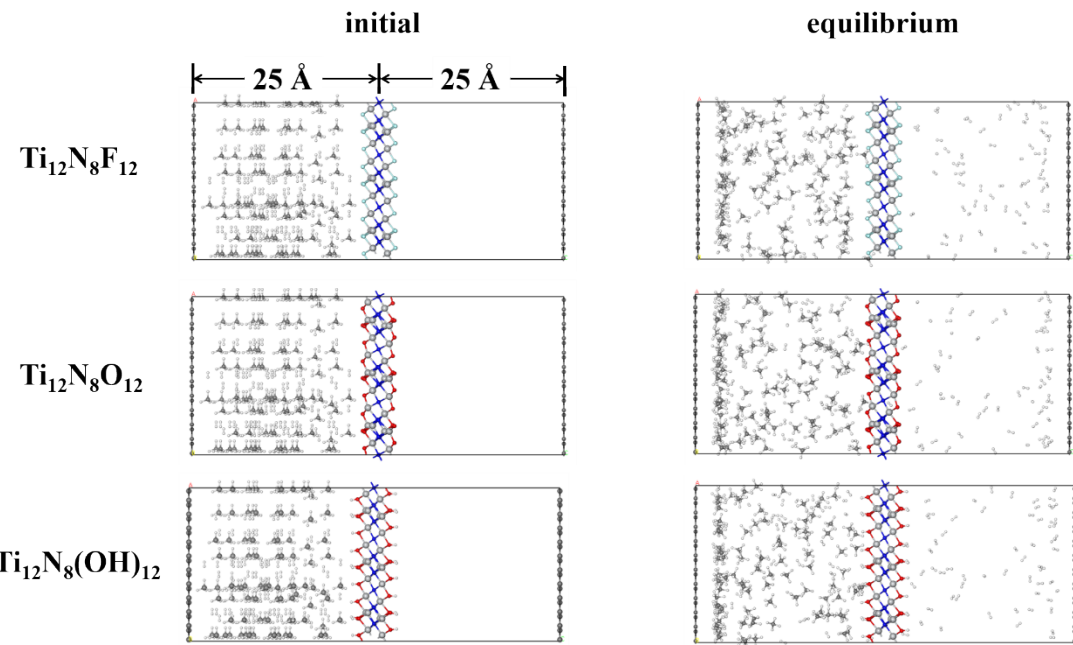


Fig. S7 Snapshots of the equimolar H₂/CH₄ mixed gases penmeating Ti₁₂N₈T₁₂ before and after 20 ns MD simulations (C, gray; O red; H, white; N blue; F, cyan)

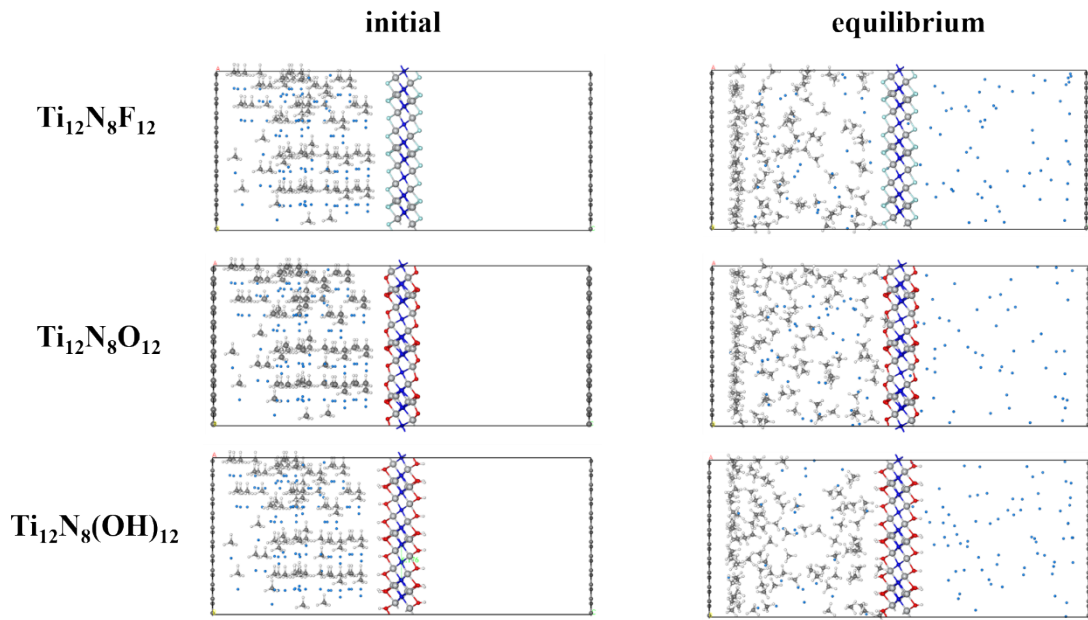


Fig. S8 Snapshots of the equimolar He/CH₄ mixed gases penmeating $\text{Ti}_{12}\text{N}_8\text{T}_{12}$ before and after 20 ns MD simulations (C, gray; O red; H, white; N blue; F, cyan; He, light blue)

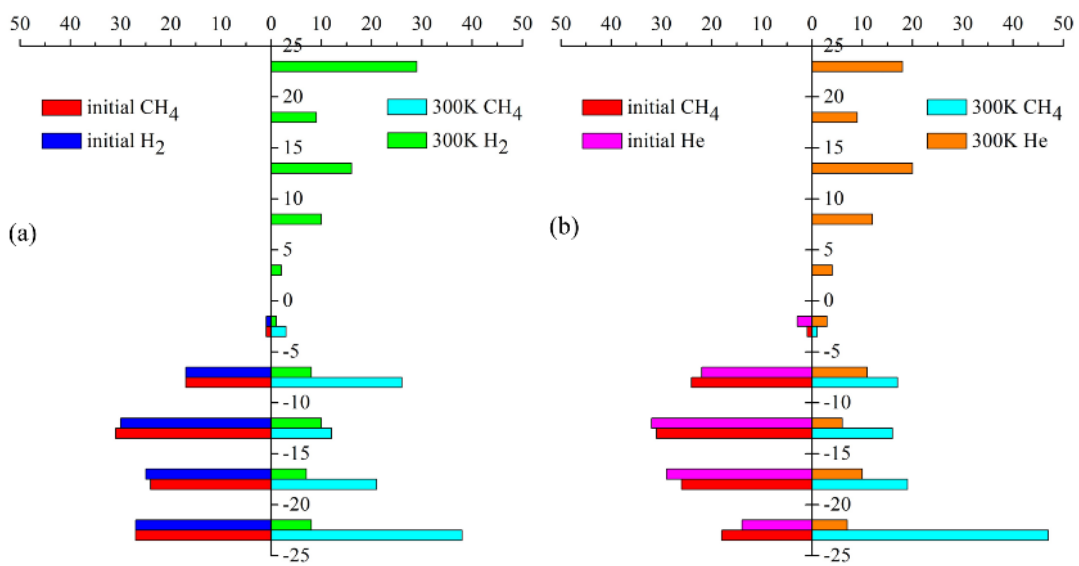


Fig. S9 Distribution of gas molecules after 20 ns MD simulations upon $\text{Ti}_{12}\text{N}_8\text{F}_{12}$

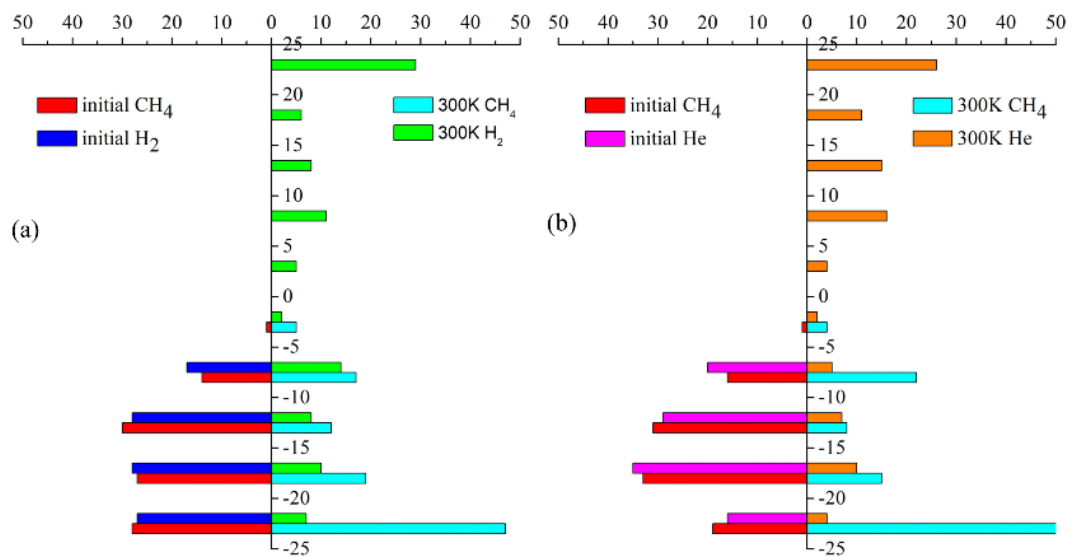


Fig. S10 Distribution of gas molecules after 20 ns MD simulations upon $\text{Ti}_{12}\text{N}_8(\text{OH})_{12}$

Table S1 Bond lengths of porous MXene Ti_{12}N_8 and $\text{Ti}_{12}\text{N}_8\text{T}_{12}$ ($\text{T} = \text{O}, \text{F}, \text{OH}$)

	Bond length (Å)						
	$\text{N}_1\text{-Ti}_1$	$\text{N}_1\text{-Ti}_3$	$\text{N}_2\text{-Ti}_1$	$\text{N}_2\text{-Ti}_3$	$\text{T}_1\text{-Ti}_1$	$\text{T}_2\text{-Ti}_2$	$\text{T}_2\text{-Ti}_1$
Ti_2N		2.070				/	
Ti_2NO_2		2.148				1.980	
Ti_2NF_2		2.059				2.145	
$\text{Ti}_2\text{N}(\text{OH})_2$		2.084				2.166	
Ti_{12}N_8	2.050	2.045	2.008	1.974	/	/	/
$\text{Ti}_{12}\text{N}_8\text{O}_{12}$	2.256	2.029	2.282	1.930	1.874	2.070	1.865
$\text{Ti}_{12}\text{N}_8\text{F}_{12}$	2.022	2.005	2.104	1.956	2.050	2.188	2.117
$\text{Ti}_{12}\text{N}_8(\text{OH})_{12}$	2.028	2.012	2.104	1.968	2.129	2.208	2.129

Table S2 Bond angle of porous MXene Ti_{12}N_8 and $\text{Ti}_{12}\text{N}_8\text{T}_{12}$ ($\text{T} = \text{O}, \text{F}, \text{OH}$)

Bond angles ($^\circ$)	Ti_{12}N_8	$\text{Ti}_{12}\text{N}_8\text{O}_{12}$	$\text{Ti}_{12}\text{N}_8\text{F}_{12}$	$\text{Ti}_{12}\text{N}_8(\text{OH})_{12}$
$\text{Ti}_1\text{-N}_1\text{-Ti}_1$	100.5	84.2	89.6	91.3
$\text{Ti}_1\text{-N}_1\text{-Ti}_3$	83.4	90.0	86.6	86.0
$\text{N}_1\text{-Ti}_1\text{-N}_2$	94.6	80.7	91.0	89.6
$\text{N}_1\text{-Ti}_3\text{-N}_2$	95.2	95.8	96.0	91.8
$\text{Ti}_1\text{-N}_2\text{-Ti}_2$	96.8	91.5	97.7	98.1
$\text{Ti}_1\text{-N}_2\text{-Ti}_4$	91.6	103.7	95.5	95.0
$\text{N}_2\text{-Ti}_1\text{-N}_2$	88.4	76.3	84.5	85.0
$\text{N}_2\text{-Ti}_2\text{-N}_2$	105.2	102.6	102.6	103.4
$\text{T}_1\text{-Ti}_1\text{-T}_1$	/	99.4	90.2	89.6
$\text{Ti}_1\text{-T}_1\text{-Ti}_1$	/	99.4	87.9	85.9
$\text{T}_1\text{-Ti}_1\text{-T}_2$	/	111.1	92.8	91.5
$\text{Ti}_2\text{-T}_2\text{-Ti}_2$	/	92.8	86.8	85.7
$\text{T}_2\text{-Ti}_2\text{-T}_2$	/	84.1	83.2	83.1
$\text{N}_1\text{-Ti}_1\text{-T}_1$	/	84.0	91.2	91.4
$\text{N}_2\text{-Ti}_1\text{-T}_1$	/	89.9	92.6	92.6
$\text{N}_2\text{-Ti}_2\text{-T}_2$	/	85.7	86.9	86.5
$\text{N}_3\text{-Ti}_2\text{-T}_2$	/	85.7	87.7	88.5

Table S3 The permeation barrier of $\text{Ti}_{12}\text{N}_8\text{T}_{12}$ ($\text{T} = \text{F}, \text{O}, \text{OH}$)

	H ₂ (meV)	He(meV)	CH ₄ (meV)
Ti ₁₂ N ₈ F ₁₂	138	48	940
Ti ₁₂ N ₈ O ₁₂	142	54	1116
Ti ₁₂ N ₈ (OH) ₁₂	143	43	850

POSCAR of Ti₁₂N₈O₁₂

Ti12N8O12

1.0

8.9134998322	0.0000000000	0.0000000000
-4.4567499161	7.7193172913	0.0000000000
0.0000000000	0.0000000000	24.4171009064

Ti	O	N
12	12	8

Direct

0.553539986	0.446460020	0.434779992
0.446460039	0.553540030	0.565220008
0.553539994	0.107079987	0.434779992
0.446460020	0.892920039	0.565220008
0.892920060	0.446460020	0.434779992
0.107080005	0.553540030	0.565220008
0.778789994	0.557590045	0.536650009
0.221210004	0.442410004	0.463349991
0.442409979	0.221199999	0.536650009
0.557590012	0.778800036	0.463349991
0.778800052	0.221210006	0.536650009
0.221200019	0.778790028	0.463349991
0.562950005	0.437050023	0.586749985
0.437049978	0.562949996	0.413250015
0.562950002	0.125900004	0.586749985
0.437050019	0.874099984	0.413250015
0.874099949	0.437049992	0.586749985
0.125900005	0.562949996	0.413250015
0.773030028	0.546049998	0.403049995
0.226970020	0.453949990	0.596950005
0.453950009	0.226979968	0.403049995
0.546049992	0.773020036	0.596950005
0.773020064	0.226970022	0.403049995
0.226979964	0.773029981	0.596950005
0.341970009	0.341970013	0.500000000
0.658030042	0.658030036	0.500000000
0.658030048	0.000000000	0.500000000
0.341970005	0.000000000	0.500000000
-0.000000006	0.658030036	0.500000000
0.000000004	0.341970013	0.500000000
0.666666670	0.333333340	0.493279977
0.333333309	0.666666617	0.506720023

POSCAR of Ti₁₂N₈F₁₂

Ti12N8F12

1.0

8.9323997498	0.0000000000	0.0000000000
-4.4661998749	7.7356851000	0.0000000000
0.0000000000	0.0000000000	23.8318996429

N	Ti	F
8	12	12

Direct

0.658510021	0.658510012	0.5000000000
0.341489964	0.341489958	0.5000000000
0.341489969	-0.0000000000	0.5000000000
0.658510031	-0.0000000000	0.5000000000
-0.000000005	0.341489958	0.5000000000
-0.000000009	0.658510012	0.5000000000
0.333333344	0.666666688	0.502960036
0.666666603	0.333333313	0.497039964
0.221369960	0.778629972	0.460660008
0.778630018	0.221369983	0.539340032
0.221369983	0.442739966	0.460660008
0.778630018	0.557260036	0.539340032
0.557259986	0.778629972	0.460660008
0.442739965	0.221369983	0.539340032
0.439590008	0.879189998	0.552279996
0.560410004	0.120809972	0.447720004
0.120809969	0.560399978	0.552279996
0.879190005	0.439600023	0.447720004
0.439600025	0.560410026	0.552279996
0.560399991	0.439590006	0.447720004
0.224930026	0.775070006	0.602779969
0.775069967	0.224929980	0.397220031
0.224929980	0.449859959	0.602779969
0.775069990	0.550139980	0.397220031
0.550140034	0.775070006	0.602779969
0.449859967	0.224929995	0.397220031
0.441549983	0.883109949	0.403400012
0.558449971	0.116890014	0.596599988
0.116889997	0.558439972	0.403400012
0.883109948	0.441559998	0.596599988
0.441559999	0.558449958	0.403400012
0.558439971	0.441549982	0.596599988

POSCAR of Ti₁₂N₈(OH)₁₂

Ti12N8O12H12

1.0

9.0165004730	0.0000000000	0.0000000000
-4.5082502365	7.8085184629	0.0000000000
0.0000000000	0.0000000000	26.5926990509

N	Ti	O	H
8	12	12	12

Direct

0.657589953	0.657589954	0.500000000
0.342410030	0.342410039	0.500000000
0.342410021	0.000000000	0.500000000
0.657589953	0.000000000	0.500000000
0.000000009	0.342410039	0.500000000
0.000000001	0.657589954	0.500000000
0.333333331	0.666666662	0.503700017
0.666666650	0.333333301	0.496299983
0.222299986	0.777699994	0.465349991
0.777700037	0.222299999	0.534649973
0.222299999	0.444599998	0.465349991
0.777699998	0.555399996	0.534649973
0.555399982	0.777699994	0.465349991
0.444600015	0.222299999	0.534649973
0.440519976	0.881039953	0.546740002
0.559480013	0.118960025	0.453259998
0.118960023	0.559480017	0.546740002
0.881039961	0.440519976	0.453259998
0.440519981	0.559480017	0.546740002
0.559480016	0.440519976	0.453259998
0.222409993	0.777589953	0.594690033
0.777590049	0.222410025	0.405309967
0.222410025	0.444820050	0.594690033
0.777589987	0.555179974	0.405309967
0.555179938	0.777590014	0.594690033
0.444820066	0.222409994	0.405309967
0.441669997	0.883329999	0.412939986
0.558329981	0.116670009	0.587059978
0.116670013	0.558340032	0.412939986
0.883329999	0.441659992	0.587059978
0.441660013	0.558330017	0.412939986
0.558340025	0.441670007	0.587059978
0.236540009	0.763459949	0.630249975
0.763459973	0.236540014	0.369750025

0.236540014	0.473080027	0.630249975
0.763459983	0.526919966	0.369750025
0.526919967	0.763459949	0.630249975
0.473080033	0.236539998	0.369750025
0.441839995	0.883689985	0.376490014
0.558160024	0.116310001	0.623510022
0.116309988	0.558149993	0.376490014
0.883689956	0.441850000	0.623510022
0.441850011	0.558160008	0.376490014
0.558150012	0.441839985	0.623510022